# Supplementary Information

## Efficient isolation and sensitive quantification of extracellular vesicles based on an integrated ExoID-Chip using photonic crystals

**Xing Dong,[a] Junjie Chi,[a] Liuzheng Zheng,[a] Biao Ma,[a] Zhiyang Li,[b] Su Wang,[b] Chao Zhao *[a] and Hong Liu *[a]**

*[a] State Key Laboratory of Bioelectronics, School of Biological Science and Medical Engineering, Southeast University, Nanjing 210096, China. E-mail: czhao86@seu.edu.cn, liuh@seu.edu.cn.*

*[b] Department of Clinical Laboratory, The Affiliated Drum Tower Hospital of Nanjing University Medical School, Nanjing 210008, China.*

### Materials and reagents

Whatman® Nuclepore™ track-etch polycarbonate membrane (13 mm diameter and 200 nm pore size) and Anodisc™ anodic aluminum oxide (AAO) membrane (13 mm diameter and 20 nm pore size) were purchased from GE Healthcare Life Science (Shanghai, China). Poly(methyl methacrylate) (PMMA) of 1 mm thick and transparent double-sided adhesive (DSA) were obtained from 3M Company (St. Paul, MN, USA). The silicone fluid (Si-fluid, DC 200, 5000 cSt) was purchased from Dow Corning (Midland, MI, USA). Monodisperse $SiO_2$ nanoparticles of different diameters were obtained from Nanjing Nanorainbow Biotechnology Co., Ltd. (Nanjing, China). Nitrocellulose was obtained from Sinopharm Chemical Reagent Co., Ltd. (Shanghai, China). Streptavidin-horseradish peroxidase (SA-HRP), streptavidin-phycoerythrin (SA-PE), bovine serum albumin (BSA), dimethylformamide (DMF), phosphotungstic acid, glutaraldehyde, acetone, ethylene alcohol, Tween-20, hydrofluoric acid (HF), hydrogen peroxide ($H_2O_2$) were purchased from Sigma-Aldrich (Shanghai, China). 10-Acetyl-3,7-dihydroxyphenoxazine (ADHP) was obtained from AAT Bioquest, Inc. (Sunnyvale, CA, USA). Mouse CD63 protein and human CD81 protein were purchased from Sino Biological Inc. (Beijing, China). Biotinylated aptamer targeting CD63 ($Apt_{CD63}$), biotinylated aptamer targeting CD81 ($Apt_{CD81}$), cell culture medium cultured from breast cancer cells and clinical samples were obtained from the Nanjing Drum Tower Hospital (Nanjing, China). Washing buffer contained 10 mM PBS and 0.20% Tween-20 (PBST). All reagents were used as received without further purification. All solutions were prepared with deionized water (18.0 MΩ cm, Milli-Q Gradient System, Millipore) with ultraviolet sterilization.

### Fabrication of ExoID-Chip device

The integrated ExoID-Chip was composed of seven layers of poly(methyl methacrylate) (PMMA, 1 mm in thickness), which was divided into two parts with a thin silicone fluid (Si-fluid) layer sandwiched in between. The upper part had an external dimension of 15 × 20 × 4 $mm^3$, which was assembled by four layers of PMMA, five layers of double-sided adhesive (DSA, 50 μm in thickness) and two filtration membranes. Similarly, the lower part had an external dimension of 15 × 36 × 3 $mm^3$, consisting of three layers of PMMA, two layers of DSA and one piece of PC nitrocellulose membrane (1mm × 2 mm × 10 μm). All of the layers containing PMMA and DSA were carved by a laser cutter (CMA4030, Han's Yueming Laser). The multilayer design drawing of the device is shown in Fig. S1. In the upper part, the first and fourth layers of PMMA both had two circular inlets with 500 μm in diameter, one for the injection of the sample while the other for the reagent channel. The second layer of PMMA had a circular chamber with a diameter of 8 mm and an injection channel with a diameter of 500 μm, the same as the third layer. Two filtration membranes with pore sizes of 200 nm and 20 nm were sandwiched between the 2nd and 3rd layers and the 3rd and 4th layers, respectively. With the assistance of the DSA for the

assembly of the integrated ExoID-Chip, chambers above the filtration membranes were used for separating and enriching EVs. For the lower part, the fifth PMMA layer had four circular holes with 500 μm in diameter. Two at the borders were outlets for waste and the other two were inlets for layers below. The sixth PMMA layer consisted of four separate circular holes with a diameter of 500 μm. The two holes on the left and those on the right were separately connected by microchannels with a width of 500 μm. There was no opening on the bottom PMMA layer. The PC nitrocellulose membrane was sandwiched between the microchannel of the sixth layer and the bottom layer. The Si-fluid thin film was evenly coated on the interface of the two parts to ensure easy sliding and prevent liquid leakage.

**Scanning electron microscopy (SEM)**

The electronic micrographs containing the opal structure of $SiO_2$ template, inverse opal photonic crystal membrane, and the filtration membranes with the pore sizes of 200 and 20 nm were observed under a scanning electron microscope (SEM, S-3000N, Hitachi). To visualize EVs captured on the filter II, the samples were treated with 2.5% glutaraldehyde for 30 min, then rinsed with PBS (10 mM, pH 7.4) and ultrapure water for 3 × 5 min to fix the EVs. The samples were then dehydrated with a graded series of ethanol (30, 50, 70, 95 and 100%) for 2 × 10 min. The dehydrated samples were coated with a gold thin film using a high-resolution ion beam coater and imaged by SEM.

**Transmission electron microscopy (TEM)**

EVs obtained from cell culture by double filtration were visualized by a transmission electron microscope (TEM, JEM-2100, JEOL). Firstly, 5 μL of purified EVs sample was dropped onto the TEM copper grid and allowed to dry naturally for 20 min. Then 5 μL of 2% phosphotungstic acid negative stain was drop onto the grid, dried for 10 min and then incubated for 30 min. The copper grids were placed under TEM for imaging afterwards.

**Dynamic light scattering (DLS) analysis**

The preparation procedures of the samples to be tested were as follows: 10 mL of cell culture media cultivated from breast cancer cells was filtered by filter I to get rid of the cell debris, and the resultant percolate was filtered by filter II and washed 3 times by 500 μL PBS solution (10 mM, pH 7.4). As a result, purified EVs were persisted on the filter II. The isolated EVs were suspended in 1 mL of PBS and characterized by dynamic light scattering (DLS) using a Malvern Zetasizer (Nano ZS, Malvern) at 25°C.

**Nanoparticle tracking analysis (NTA)**

To measure the concentration of EVs in clinical samples, containing serum from breast cancer patients and healthy individuals, we used a nanoparticle tracking analysis (NTA) system (PMX 110, ZetaView). Briefly, 1 mL of sample (obtained by 100 μL of serum diluted by 10 times) was filtered by filter I, then the resultant percolate was filtered by filter II and washed 3 times with 500 μL PBS solution (10 mM, pH 7.4). As a result, purified EVs were trapped on the filter II. The isolated EVs were resuspended in 100 μL of PBS and the concentration was measured with NTA. All NTA measurements were conducted using identical settings to ensure consistent results.

**Fluorescence enhancement effect of resorufin on different PC membranes**

The emission band of resorufin (9-hydroxy-3-isophenoxazone) generated from ADHP oxidation presented a peak at 583 nm ($\lambda_{em}$) under excitation wavelength of 570 nm ($\lambda_{ex}$). To evaluate effects of stopband

position on the fluorescence enhancement of resorufin, we dropcast 1 μL of solution containing 100 μM fluorogenic substrate (ADHP) and $H_2O_2$, and 10 μg/mL SA-HRP onto 1 × 2 $mm^2$ rectangular nitrocellulose membranes including nonporous membrane and different PC membranes. After reacting at 25°C in the dark for 15 min, the fluorescence images on the PC membranes were obtained by a fluorescence microscope (SZX16, Olympus) equipped with CCD camera (MicroPublisher 5.0 RTV, QImaging). The fluorescence intensity values were represented by the gray values of the detection area acquired by ImageJ software.

**Characterization of nonspecific binding**

To estimate the nonspecific binding during the EV analysis, the negative and positive control experiments were designed and conducted in parallel. In parallel experiments, 200 μL of the cell medium cultured from breast cancer cells at concentration of 1 × $10^7$ EVs/mL was injected into the ExoID-Chip. The operation process was as follows: in the Sample I, as the positive control, the CD63-coated PC membrane was assembled into the device, and each reaction solution was injected into the ExoID-Chip as described in the experimental section; in the Sample II, the uncoated PC membrane was assembled into the device, and each reaction solution was injected into the device the same as in the Sample I; in the Sample III, the CD63-coated PC membrane was assembled into the device, and the aptamer was replaced by PBS buffer (10 mM, pH 7.4), and other operating procedures were the same as in the Sample I; in the Sample IV, the CD63-coated PC membrane was assembled into the device, and the SA-HRP was replaced by PBS buffer (10 mM, pH 7.4), and other operating procedures were the same as in the Sample I. All fluorescence results were obtained by the fluorescence microscope (SZX16, Olympus) equipped with CCD camera (MicroPublisher 5.0 RTV, QImaging).

**Characterization of unsuccessful binding**

To characterize the unsuccessful binding, 200 μL of the EVs sample derived from breast cancer cell culture medium at concentration of 1 × $10^7$ EVs/mL was injected into the ExoID-Chip device. Then the operation process was as follows: in the Sample I, 200 μL of PBS buffer (10 mM, pH 7.4) was injected into the device; in the Sample II, 200 μL of 500 nM $Apt_{CD63}$ was fed into the device to combine with EVs trapped on the filter II. After flushing with 100 μL of PBS solution (10 mM, pH 7.4) containing 0.20% Tween-20, the ExoID-Chip device was then air-dried to completely remove residual liquid. The filter II of Sample I and II were taken out from the device, and then reacted with 40 μL of biotinylated aptamer (500 nM) for 20 min. After washing the filters of Sample I and II with 10 mM PBST buffer (pH 7.4) for three times, 40 μL of SA-PE (20 μg/mL) was added on the filters of Sample I and II to combine with the biotinylated aptamer. After interaction for 15 min, the fluorescence intensity on the filter II of sample I and II were observed by the fluorescence microscope (SZX16, Olympus) equipped with CCD camera (MicroPublisher 5.0 RTV, QImaging).

**Reproducibility and stability analysis**

To investigate the reproducibility and stability of the ExoID-Chip device, breast cancer cell culture medium on the EVs concentration of 1 × $10^7$ EVs/mL were analysed 5 times in parallel following the procedure described in the experimental section. All fluorescence results were obtained by the fluorescence microscope (SZX16, Olympus) equipped with CCD camera (MicroPublisher 5.0 RTV, QImaging).

Table S1 Workflow of ExoID-Chip Device

| | Scheme | Injectant | Volume | Duration | |
|---|---|---|---|---|---|
| Step 1 | 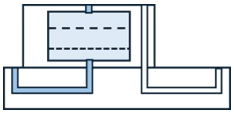 | cell culture or serum<br><br>PBST (10 mM, pH 7.4, 0.20% Tween-20)<br><br>Air | 200 µL<br><br>100 µL<br><br>100 µL | 40 min | 119 min |
| Step 2 | 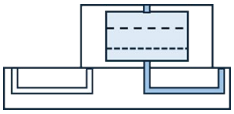 | $Apt_{CD63}$<br><br>PBST (10 mM, pH 7.4, 0.20% Tween-20)<br><br>Air | 200 µL<br><br>100 µL<br><br>100 µL | 40 min | |
| Step 3 | 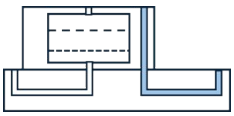 | SA-HRP<br><br>PBST (10 mM, pH 7.4, 0.20% Tween-20) | 20 µL (interaction for 15 min)<br><br>50 µL | 22 min | |
| | | Fluorogenic substrate ($ADHP+H_2O_2$) | 20 µL (incubate for 15 min) | 17 min | |

Table S2. Results of Mann-Whitney U test of the difference between the healthy controls and breast cancer patients.

| EVs Marker | Healthy controls/Patients | |
|---|---|---|
| | $\Delta I$ | NTA |
| CD63 | $p$=0.003 | P=0.004 |
| CD81 | P=0.003 | |

Significance level was set at $p < 0.05$.

Table S3 Comparison of currently available microfluidic platforms for EV analysis.

| EV isolation | Detection | Device performance | | | Ref. |
|---|---|---|---|---|---|
| | | Sample size | Time | Sensitivity (LOD) | |
| Size-exclusion | N/A | 10~100 μL | < 3 h | N/A | 1 |
| Electrophoresis | N/A | N/A | 20 min | N/A | 2 |
| Immuno-capure (IC) based on affinity pulldown | Exosome Lysis | 10 μL | N/A | N/A | 3 |
| Immunomagnetic capture (IMC) | Exosome lysis & ELISA | 30 ~150 μL | ~100 min | N/A | 4 |
| Immunoaffinity | Fluorescent staining | 400 μL | ~70 min | 0.5 pM | 5 |
| Electrohydrodynamic flow assisted IC | Colorimetric ELISA | N/A | ~120 min | 2760 $\mu L^{-1}$ | 6 |
| IMC | Immunostaining | 20 μL | 40 min | 750 μL-1 | 7 |
| Immunoaffinity | Fluorogenic ELISA | 2 μL | N/A | 50 $\mu L^{-1}$ (80aM) | 8 |
| Magnetic immunoaffinity | Electrochemical assay | 10 μL | 1 h | 30 $\mu L^{-1}$ | 9 |
| immunocapture | Fluorogenic ELISA | 2 μL | N/A | 10 $\mu L^{-1}$ | 10 |
| Size-exclusion | Fluorogenic ELISA | 20 μL | 119 min | 8.9 $\mu L^{-1}$ | This work |

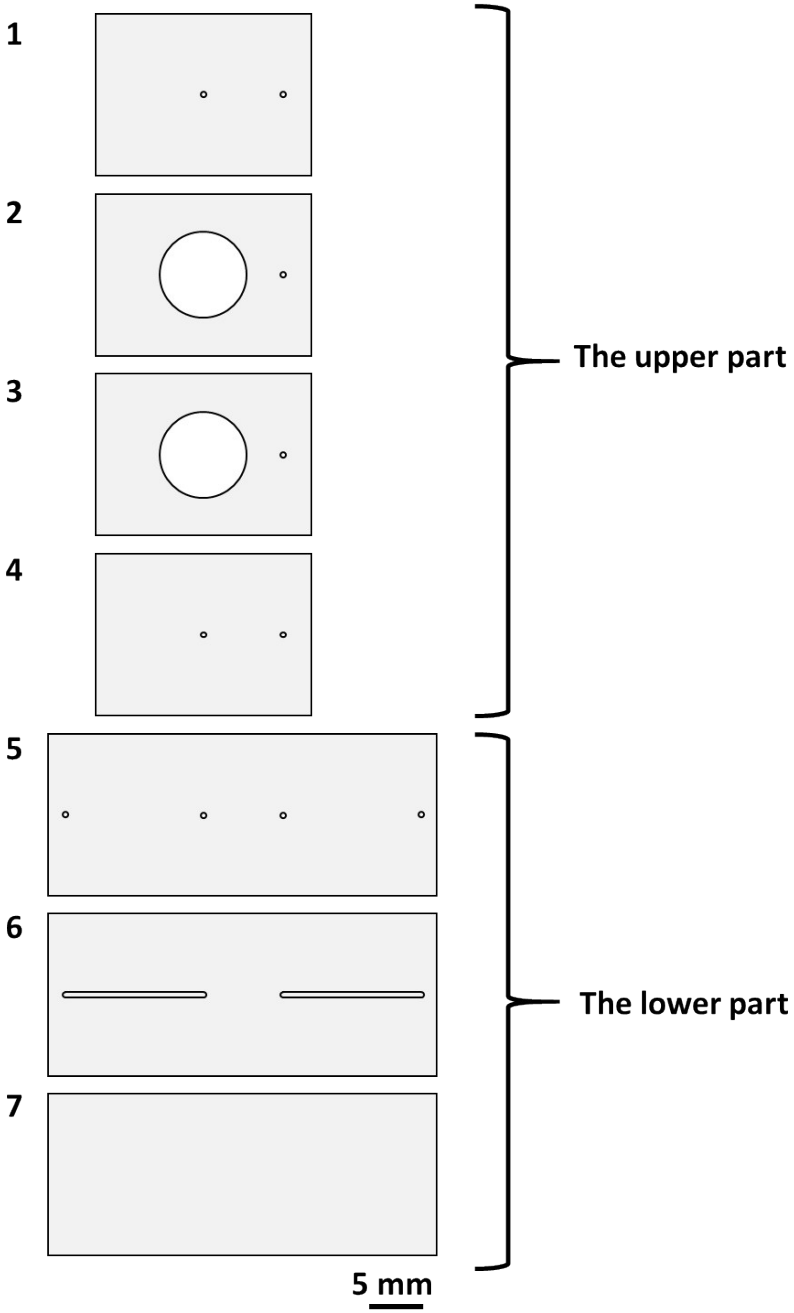


Figure S1. Expanded view of the ExoID-Chip showing the seven layers of the PMMA. Scale bar: 5mm.

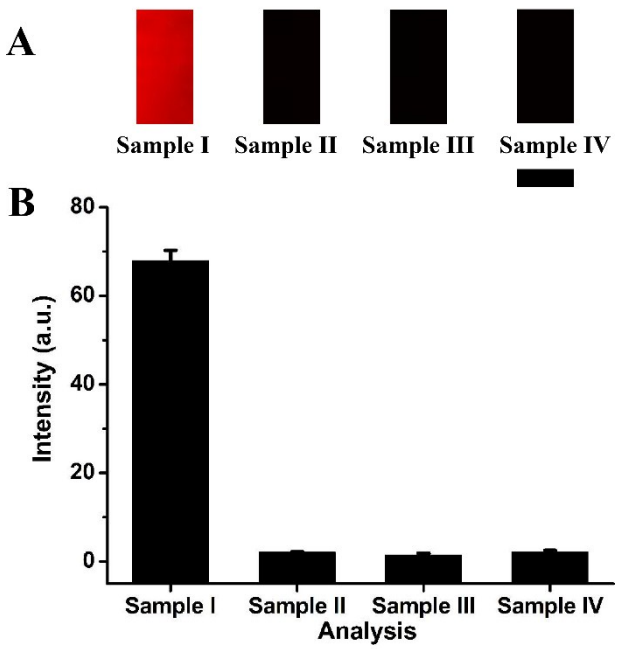


**Fig. S2** (A) Fluorescence micrographs of ADHP catalyzed by SA-HRP binding excessive $Apt_{CD63}$ which were captured by the CD63 on the PC membrane. Sample I: CD63+$Apt_{CD63}$+SA-HRP+ADHP. Sample II: $Apt_{CD63}$+SA-HRP+ADHP. Sample III: CD63+SA-HRP+ADHP. Sample IV: CD63+$Apt_{CD63}$+ADHP. Sample II, Sample III, and Sample IV lacked CD63, $Apt_{CD63}$ and SA-HRP in the analysis process, respectively. Scale bar: 500 μm. (B) Fluorescent intensity measured with error bars indicating standard deviations for Sample I, II, III and IV.

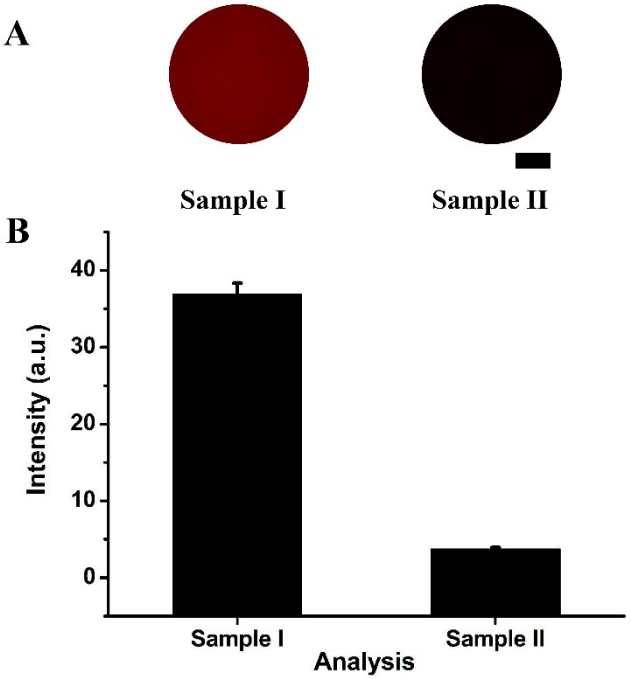


**Fig. S3** (A) Fluorescence micrographs of SA-PE on the filter II. Scale bar: 2 mm. (B) Fluorescent intensity measured with error bars indicating standard deviations for Sample I and II.

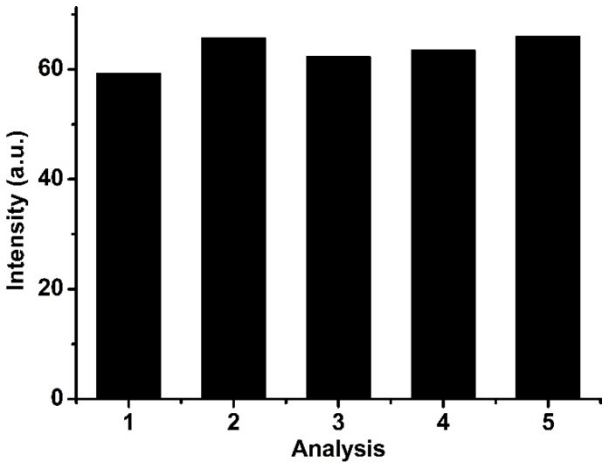


**Fig. S4** Variability data for EV analysis of 5 times on the EVs concentration of $1 \times 10^7$ $mL^{-1}$ (RSD= 4.3%, n = 5).

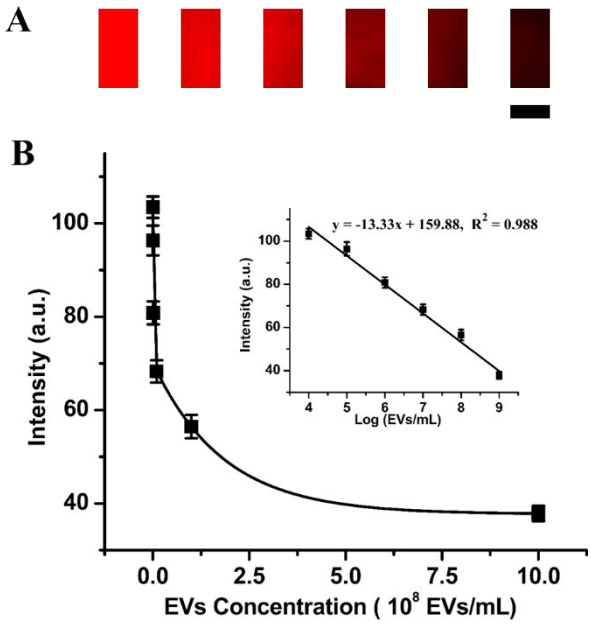


**Fig. S5** (A) Fluorescence detection of samples containing breast cancer cell culture derived EVs in PBS at different concentrations with CD81 as the binding site (left to right: $1 \times 10^4$ to $1 \times 10^9$ EVs/mL). Scale bar: 500 µm. (B) Fluorescence intensity measured after completion of the bioassay as a function of the concentration of EVs in the breast cancer cell culture. Inset: the fluorescence intensity as a function of the logarithm of the EVs concentration. Error bars represent the standard deviation of three independent experiments (RSD = 4.4%, n = 3).

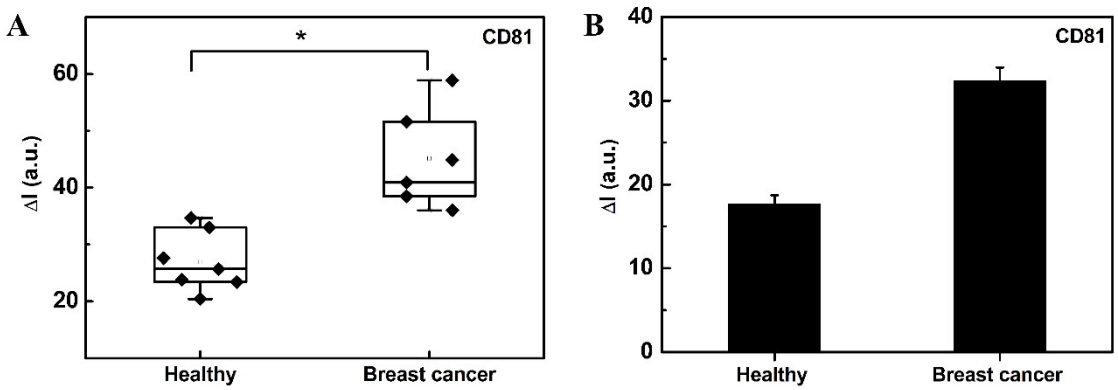


**Fig. S6** (A) Clinical validation of EVs derived from serum with CD81 as the binding site for differentiating breast cancer patients from healthy individuals. The detection signal Δ*I* from serum samples collected from patients with breast cancer (n = 6) and healthy people (n = 7) were detected with ExoID-Chip device and compared in a box-plot showing higher signal of EVs from patients compared to healthy controls. A Mann-Whitney U test was used to analyze the statistical difference between the two groups. The asterisk (*) indicates statistical significance ($p < 0.05$). (B) The expression level of CD81 on EVs from serum of breast cancer patient and healthy individual at same number of EVs ($1.3 \times 10^7$ EVs/mL counted by NTA). Error bars were from three repeated measurements.

**References**


1. F. Liu, O. Vermesh, V. Mani, T. J. Ge, S. J. Madsen, A. Sabour, E. C. Hsu, G. Gowrishankar, M. Kanada, J. V. Jokerst, R. G. Sierra, E. Chang, K. Lau, K. Sridhar, A. Bermudez, S. J. Pitteri, T. Stoyanova, R. Sinclair, V. S. Nair, S. S. Gambhir and U. Demirci, *ACS Nano*, 2017, **11**, 10712-10723.
2. S. Marczak, K. Richards, Z. Ramshani, E. Smith, S. Senapati, R. Hill, D. B. Go and H. C. Chang, *Electrophoresis*, 2018, DOI: 10.1002/elps.201700491.
3. X. N. Fang, Y. K. Duan, G. B. Adkins, S. Q. Pan, H. Wang, Y. Liu and W. W. Zhong, *Anal. Chem.*, 2018, **90**, 2787-2795.
4. M. He, J. Crow, M. Roth, Y. Zeng and A. K. Godwin, *Lab Chip*, 2014, **14**, 3773-3780.
5. S. S. Kanwar, C. J. Dunlay, D. M. Simeone and S. Nagrath, *Lab Chip*, 2014, **14**, 1891-1900.
6. R. Vaidyanathan, M. Naghibosadat, S. Rauf, D. Korbie, L. G. Carrascosa, M. J. Shiddiky and M. Trau, *Anal Chem*, 2014, **86**, 11125-11132.
7. Z. Zhao, Y. Yang, Y. Zeng and M. He, *Lab Chip*, 2016, **16**, 489-496.
8. P. Zhang, M. He and Y. Zeng, *Lab Chip*, 2016, **16**, 3033-3042.
9. S. Jeong, J. Park, D. Pathania, C. M. Castro, R. Weissleder and H. Lee, *ACS Nano*, 2016, **10**, 1802-1809.
10. P. Zhang, X. Zhou, M. He, Y. Q. Shang, A. L. Tetlow, A. K. Godwin and Y. Zeng, *Nat. Biomed. Eng.*, 2019, 3, 438-451.